2024 IEEE International Conference on Robotics and Automation (ICRA 2024)
May 13-17, 2024. Yokohama, Japan

Leaf-Inspired FSR Array and Insole-Type Sensor Module for Mobile Three-Dimensional Ground Reaction Force Estimation

Taeyeon Kim[1], Eunseok Song[1], Seongbin An[1], Hyunjin Choi[2], and Kyoungchul Kong[1]

***Abstract*— This paper presents an insole-type sensor module with a novel leaf-inspired force-sensitive resistor (FSR) array for accurate three-dimensional ground reaction force (GRF) estimation during human's various motions. Joint torque analysis, essential for numerous applications in biomechanics and wearable robotics, necessitates the measurement of three-dimensional GRF vector information, traditionally achieved in indoor environments using costly force plates. To overcome these limitations, this study proposes an alternative method by incorporating FSRs on three inclined planes within the insole. A vector scaling process transforms the force values from the FSRs into the three-dimensional force vector, enabling continuous and user-independent estimation of GRF. The sensor module is integrated with machine learning, demonstrating its accuracy and usability in various motion scenarios. The results confirm the effectiveness of the leaf-inspired FSR array, giving the possibilities for portable and cost-effective motion analysis systems.**

I. INTRODUCTION

In the analysis of human walking and running motions, joint torque is an indispensable physical quantity and only derivable by inverse dynamics. The joint torque information can be utilized in various applications such as human motion efficiency analysis [1], [2], reference of the control strategy in wearable robots [3]–[8], and performance analysis of wearable robots for industry or rehabilitation [9]–[11]. While solving the inverse dynamics, not only joint angles but also three-dimensional GRF(Ground Reaction Force) and COP(Center of Pressure) information is required, and the most common method to measure them is using costly force plates. Using more than two force plates is necessary to measure a single stride. In other way, treadmills with built-in force plates have been developed, enabling continuous gait measurements.

However, with the installed equipment listed above, the measurements are limited to indoor environments and motions that are only achievable on the treadmill. To overcome the disadvantage of expensive and space-limited equipment, incorporating sensors into shoes was alternatively proposed for motion analysis. In particular, insole-type sensors place pressure sensors inside pad-like inserts to estimate the GRF vector. They have the advantage of being usable regardless of shoe type or shape. At first, insole-type sensors previously proposed have only measured force in a vertical direction [12], or COP [13] using thin force-sensitive resistors(FSR) by using least square regression. This is due to the insole's low thickness, which makes it difficult to measure shear stress between the sole of the foot and the ground. To estimate the shear stresses, some studies have employed deep learning techniques [14], [15]. However, since it is one-dimensional, it excels in estimating GRF in the vertical direction but has low accuracy in other directions. The absence of directly related information is one of the reasons, but more importantly, the shear stress distribution inevitably varies with each motion and often varies between individuals. Therefore, the accuracy of user-independent and random shear stress estimation is particularly low. Estimating three-dimensional data from one-dimensional data easily leads to over-fitting problems, and will amplify the errors above.

Fig. 1. A proposed leaf-inspired FSR array

Demand for a method that directly measures three-dimensional forces using sensors rises. These include methods for both insole and outsole types, such as attaching electrical conductive rubber in all areas [16], incorporating optical sensors with fast response times and no hysteresis into insoles [17], [18], embedding force sensors in cells with special shapes, measuring capacitance based on deformation caused by uniquely designed shapes [19], [20], or design a MEMS sensor that measures three-dimensional force [21]. While it may seem that measuring shear forces on a plane requires two pairs or four sensors, there have been studies that have shown it is possible with three sensors [22].

The leaves of common plants have a unique geometric arrangement that allows them to maintain photosynthesis even when the direction of sunlight changes, as shown in Fig. 1. In this study, a novel leaf-inspired arrangement for FSR is proposed and implemented in the insole-type sensor module. By placing FSRs on three different inclined planes and shaping them into small coin forms, it is enable to measure

*This work was supported by the National Research Foundation of Korea (NRF) grant funded by the Korea government (MSIT) (No. 2022R1A3B1077880).

[1]The authors are with Exoskeleton Laboratory, the Department of Mechanical Engineering, Korea Advanced Institute of Science and Technology (KAIST), 291, Daehak-ro, Yuseong-gu, Daejeon, Republic of Korea ty.kim, eunseok.song, sbin, kckong@kaist.ac.kr

[2]The author is with the Department of Human Intelligence and Robot Engineering, Sangmyung University, 31, Sangmyeongdae-gil, Dongnam-gu, Cheonan-si, Chungcheongnam-do, Republic of Korea hyunjin@smu.ac.kr

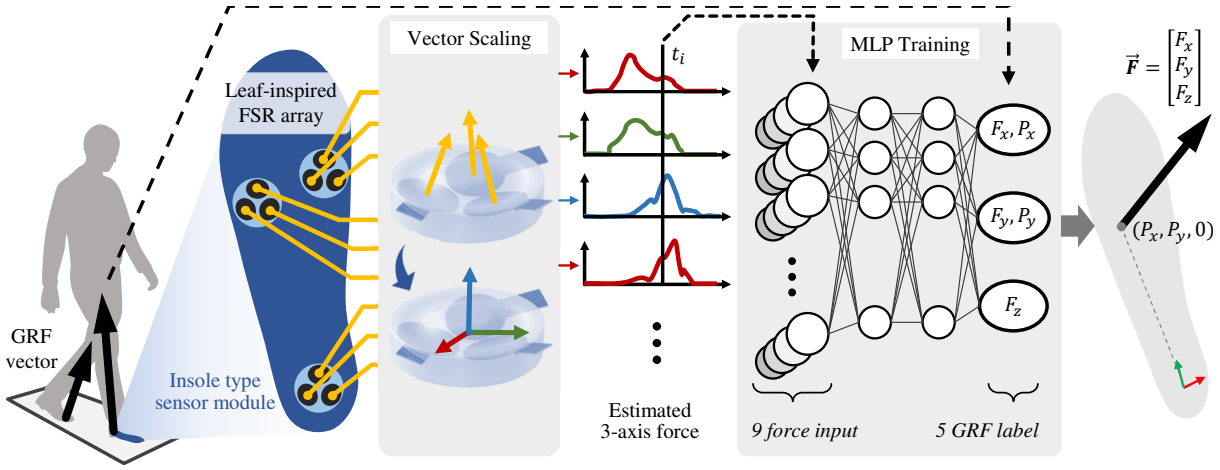

Fig. 2. Schematic illustration of the GRF and COP estimating process with the proposed leaf-inspired FSR array. The measured force value from FSR will be transformed to the three-dimensional force value by the linear geometric relationship. Using the estimated three-dimensional force as inputs and the measured GRF and COP value as labels of the MLP network, the proposed insole type sensor can precisely estimate the ground reaction forces.

three-dimensional force. The entire process of estimating GRF and COP is illustrated in Fig. 2. Three leaf-inspired FSR arrays are located in the insole-type sensor module contains. The fabrication and thickness optimization of the proposed sensor module will be discussed in Section 2-A. The measured forces from three FSRs will be calibrated, linearized, and transformed into the three-dimensional force vector. This process is called vector scaling and is described in Section 2-B. Another important feature is the continuity between the estimated three-dimensional force vectors and the total GRF vector of a single foot. Thus, in Section 3, the manufacturing process of the insole-type sensor module and an MLP network was introduced. The experiment process for collecting the data and validating the sensors is explained in Section 4. After constructing the network using the data, the accuracy of estimating GRF and COP during various mobile situations at different speeds was verified. This study concludes by confirming the usefulness of the leaf-inspired FSR array proposed in this research and discussing the results.

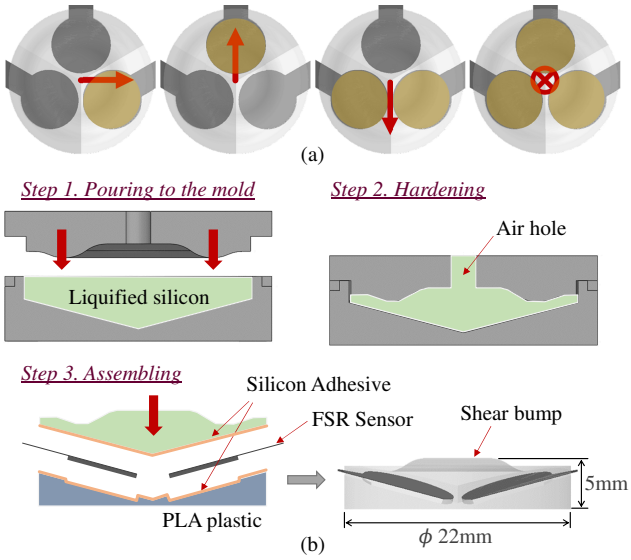

Fig. 3. Concept and fabrication of array. (a) A conceptual principle of the leaf-inspired FSR array, (b) fabrication process and dimensions.

II. LEAF-INSPIRED FSR ARRAY

A. Concept and fabrication of array

Inspired by the geometric arrangement of leaves, each FSR is tilted toward the center of the array. As shown in Fig. 3(a), at least one FSR will be pressed regardless of the direction of the applied force. Even if the planes are not orthogonal with each other, as long as three linearly independent normal vectors exist, the three-dimensional force with respect to Euclidean coordinates can be calculated. Therefore, the number of sensors was selected as three, arranged at 120° intervals. To maintain the proposed arrangement, the FSRs are inserted between thoroughly designed silicon forms and 3D printed PLA plastic as shown in Fig. 3(b). The shape of the assembled body that surrounds the FSRs is designed to have a flat bottom surface and a shear bump at the center of the top surface. Due to the presence of a bump on the upper surface, the applied force can be concentrated in the center, and the shear component of the force is better transmitted to each plane. Since FSRs can only measure positive force, if force is applied in the negative direction, the measurement value will be equivalent to the zero-force state. Thus the proposed sensor can only estimate vectors within the triangular concave range formed by the three planes. The FSRs were from Interlink Electronics, model FSR-UX400Short, with an active area of 5.62mm in diameter. The linear force measurement range of the sensor is 0.5N to 150N. Although the force range mentioned above may be somewhat limited for measuring GRF, when converted to pressure by dividing by the active area of the FSR, it reaches a maximum of approximately 3300kPa, which is sufficient to withstand the maximum pressures generated during daily life.

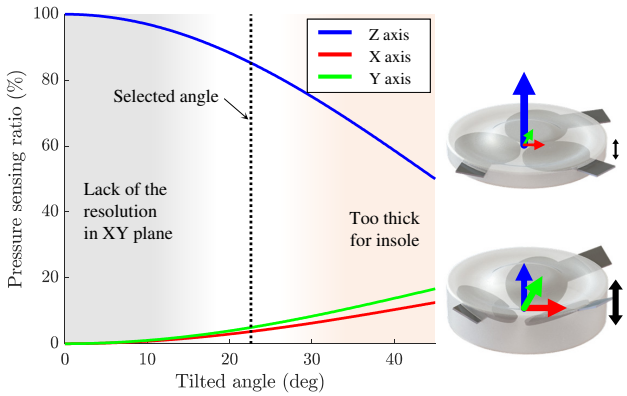

Fig. 4. Thickness selection for insole application while considering three-dimensional force sensing resolutions.

The force sensing ratio at each axis can be calculated when force is applied to the upper surface. Fig. 4 illustrates the variations in force ratios with respect to the tilted angles. If the sensor module is too thin, the angles of the three planes would be too small, resulting in insufficient resolution for the shear force. If the sensor module is too thick, the insole will also need to be thicker, potentially causing the shoe to fit too tightly. Therefore, the resolution ratio between the sum of XY plane and the Z-axis was selected as 10:1, which the corresponding angle is 22.6°. The minimum thickness of 5mm was selected as the final thickness to fully cover the FSR arrays.

B. Vector scaling for force estimation

As illustrated in Fig. 2, the objective is three-dimensional GRF estimation by measured force values from FSRs on an insole. Previous studies proposing sensors capable of measuring three-dimensional forces assumed linear relationships and estimated true values from measured values through least-square regression. However, the potential nonlinearity will be ignored with this regression. Machine learning is an effective alternative to overcome these existing limitations. If there is a sufficiently deep and wide network, all necessary processes for estimating the GRF from the raw data, such as unit conversion, nonlinear characteristics, and force estimation in the sensor-less region, can be included within the network. However, in real-time online estimation applications, higher computing power will be required to maintain estimation speed as the network becomes larger. Conversely, as the input of the network exhibits a higher correlation with the information to be estimated, even a smaller network with only a few hidden layers can stably improve estimation accuracy by performing loss minimization. Therefore, to increase physical correlation, a vector scaling process is introduced, allowing the proposed sensor module to estimate the configuration of the applied three-dimensional force close to the actual values.

First of all, curve-fitting is required to enable the direct estimation of the force applied vertically to the FSR. The FSR, which is a resistor, exhibits an exponential relationship with force when configured in a simple voltage divider circuit.

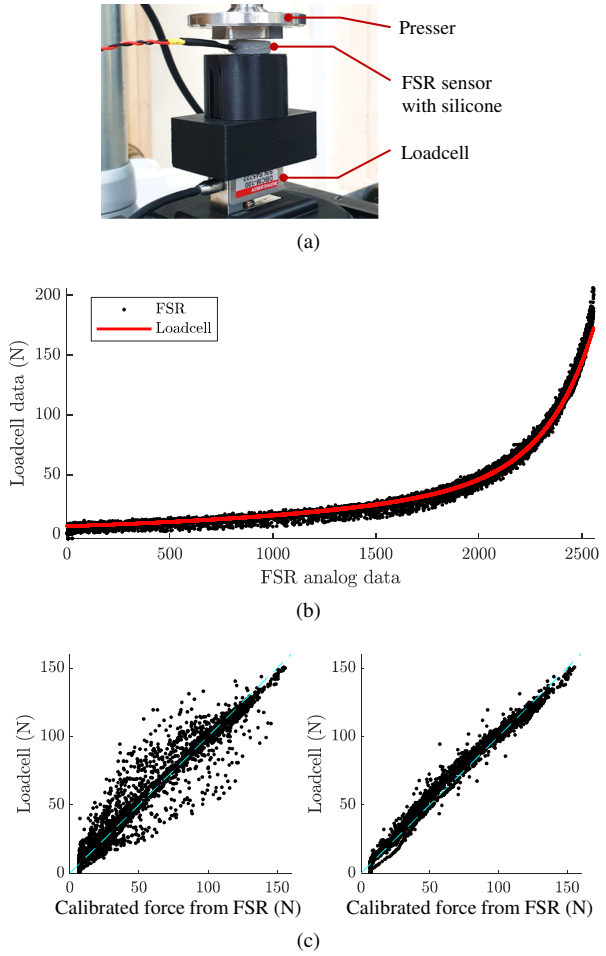

Fig. 5. Data for linearization process. (a) FSR analog data and loadcell data while applying quasi-static force. (b) Loadcell and calibrated FSR's data in various frequencies. (c) Plot before and after applying the lag compensator.

To compensate for this, the coefficients of the function are numerically solved to represent the actual force in terms of analog measurement values by using the following equation:

$$y = c_1 \exp(c_2 x) + c_3 \exp(c_4 x). \tag{1}$$

where x is the FSR's analog signal, and y is measured force from the loadcell. Utilizing a prismatic presser that ensures unidirectional motion, quasi-static force in a sufficient range was applied as shown in Fig. 5(a). Obtained data and the curve of equation (1) are plotted in Fig. 5(b). Following the curve-fitting calibration, the unique viscoelasticity of the silicon used to form the sensor array is reflected in the sensor output, resulting in hysteresis in the measurements. A lag compensator was designed, taking into account the characteristics of the GRF and selecting an appropriate frequency range, as described below:

$$F_{\text{Load}} = \frac{1+as}{1+bs} F_{\text{FSR}}, \tag{2}$$

where $a = 0.0012$ and $b = 0.008$ for setting the lagging frequency range around 50Hz. It can be observed from Fig. 5(c) that the linearization has been achieved for the force applied at various frequencies.

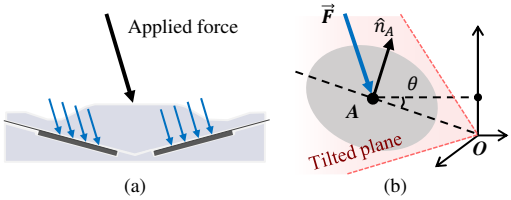

Fig. 6. While pressing the array, all force vector is assumed to have the same direction as (a), and force vector will form a specific angle with the normal vector of each plane (b).

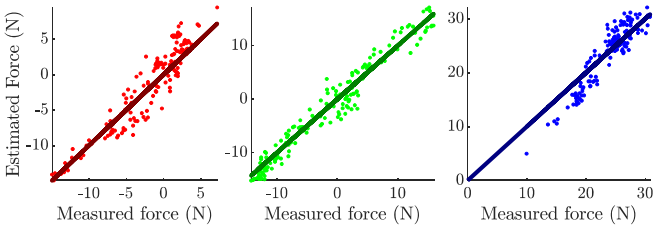

Fig. 7. Three-dimensional force estimation performance of a single FSR array by vector scaling.

Once the analog signals of the FSR are calibrated to the actual forces, a process is required to convert the measured three forces into the three-dimensional force vectors. Since the diameter of the silicone shape is sufficiently small compared to the width of the sole, the direction of the force applied to the entire upper surface can be assumed as the same as to each FSR, as 6(a). Let's denote the three planes where the sensors lie as A, B, and C, with their corresponding normal vectors as $\hat{n}_A$, $\hat{n}_B$, and $\hat{n}_C$, respectively. 6(b) illustrates a representation specifically for plane A for better comprehension. When the plane is inclined by an angle θ relative to the sensor's bottom surface, the normal vector for each plane can be determined as follows:

$$\hat{n}_A = \begin{bmatrix} 0 & \sin\theta & \cos\theta \end{bmatrix}^T, \tag{3}$$

$$\hat{n}_B = \mathbb{R}_Z(2\pi/3)\ \hat{n}_A, \tag{4}$$

$$\hat{n}_C = \mathbb{R}_Z(4\pi/3)\ \hat{n}_A. \tag{5}$$

where $\mathbb{R}_Z(\theta)$ is a rotation matrix with respect to z-axis. Under the assumption of uniform direction, the force values applied to each plane can be regarded as the vector projection of the force $\vec{F} = \begin{bmatrix} F_x & F_y & F_z \end{bmatrix}$ on the normal vector. In this case, the force $\vec{F}$ is limited in the concave range formed by the three planes. When the FSR measures the force values as F_A, F_B, and F_C on each plane,

$$\vec{F} \cdot \hat{n}_i = F_i \text{ for } i = A, B, C. \tag{6}$$

The result of formulating equations for three sensors and solving them simultaneously is as follows:

$$F_x = \frac{\sqrt{3}\left(\tan^2(\theta/2)+1\right)(F_B - F_C)}{6\tan(\theta/2)}, \tag{7}$$

$$F_y = \frac{\left(\tan^2(\theta/2)+1\right)(2F_A - F_B - F_C)}{6\tan(\theta/2)}, \tag{8}$$

$$F_z = -\frac{\left(\tan^2(\theta/2)+1\right)(F_A + F_B + F_C)}{3\left(\tan^2(\theta/2)-1\right)}. \tag{9}$$

By utilizing the above linear relationships, it is possible to estimate the three-dimensional force vector using the FSR measurements. The performance of the vector scaling process is illustrated in Fig. 7.

III. INSOLE SENSOR MODULE FOR GRF ESTIMATION

A. Design and manufacture process of the sensor system

Considering the statistical pressure distribution to foot soles during human gait, leaf-inspired FSR arrays were placed at the positions of the heel, 1st and 5th metatarsal [23]. The fabrication process of the insole sensor module is shown in Fig. 8(a). Insoles that were 2mm thick were prepared, and the location for the wires was carefully carved out. The holes were drilled at the positions where the FSR array would be placed. Subsequently, to prevent the sensor from detaching during repeated use and to minimize any discomfort due to foreign objects, a thin adhesive film was applied on both sides of the insole sensor module. This process ensured that the insole sensor module maintained the same thickness as the silicon shape, providing durability and comfort during extended use.

B. Data acquisition experiment for GRF estimation network

The aim of this study was to estimate the GRF and COP on each foot using supervised learning. To achieve this, the necessary input and label data were acquired. In indoor environments, the position of COP can be measured with respect to the fixed ground coordinate. However, in outdoor environments, to facilitate future inverse dynamics analysis, a coordinate system has to be defined with the origin at the ankle joint and fixed on the foot. For this, obtained data from indoor devices is transformed into this foot coordinate, allowing for the estimation of the relative COP positions using the proposed sensor module.

The main data collection experiment protocol was designed to ensure that the resultant network would not overfit to specific scenarios, but rather exhibit adaptability to a wide array of situations. The protocol is started with standing straight, to check the natural pressure distribution of the participant by their own foot sole shape. This distribution to nine different FSR sensors is used for the post-calibration. Then, the experiment protocol involved walking at deviations from the average walking speed, collecting data for 30 seconds at each speed (0.75, 1, 1.25 m/s). Additionally, unconventional movements such as stepping in random directions, abnormal walking(shaking body, tip-toeing, walking with heels only, changing every step's foot direction), and squatting were incorporated to establish a comprehensive and robust correlation with the data labels, thus preventing an excessive tendency to conform to specific gait patterns. Throughout these experiments, measurements were taken, including raw data from FSR sensors, vector scaling results from each FSR array, GRF and COP measurements from the AMTI tandem force plate treadmill, and positions of the markers attached on the foot obtained through VICON

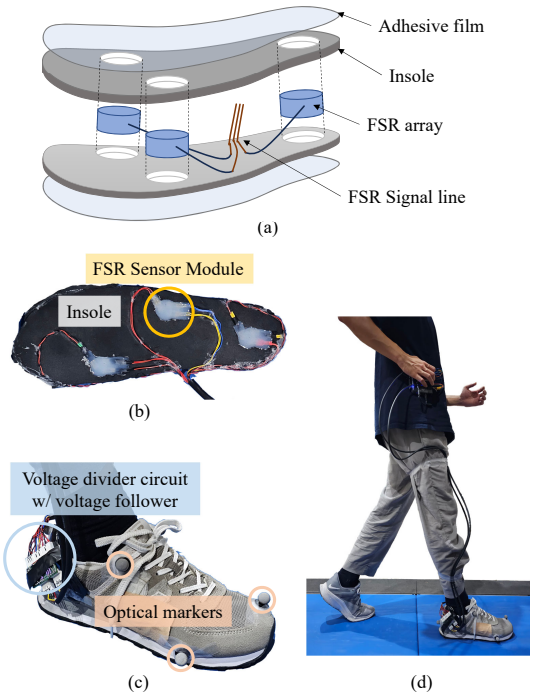

Fig. 8. (a) Schematic diagram of the insole module fabrication process. (b) Fabricated insole-type sensor system. (c) Experiment setup with the sensor data acquisition and the optical markers. (d) Level walking experiment.

motion capture system. The FSRs and force plate data were measured at 1000 Hz sampling frequency, while the marker position was measured at 250 Hz and post-interpolated. Due to inherent noise in the force plate measurements, a fifth-order lowpass filter with a cutoff frequency of 45Hz was employed to achieve a smoother gradient descent during the network learning process.

The aim was to maximize the physical correlation between the input and the ground truth to minimize the network's layers. Thus, the network architecture is chosen to be sufficiently lightweight for real-time online estimation applications, such as mobile networks for wearable devices [24], [25]. Unlike the papers dealing with time-series data, a time window was not employed, since the core purpose of this sensor module is getting GRF and COP at the exact moment, regardless of the type of motion. Consequently, a simple Multi-Layer Perceptron (MLP) was implemented, and the network consists of only two short hidden layers of $9 \times 512 \times 512 \times 5$, with basic batch normalization and ReLU activation. After separating the training sets and validating sets of each trial, all training sets from different types of motions are used to obtain a single network. For comparison, another network which is learned with only Z-axis information is prepared.

TABLE I

RMS ERROR OF THE ESTIMATION RESULT USING LEAF FSR ARRAY.

Motion type	Info. type	F_x (N)	F_y (N)	F_z (N)	P_x (mm)	P_y (mm)
Abnormal gait	Leaf	12.31	13.44	31.77	3.64	8.87
	Z axis	32.32	37.56	66.77	6.93	10.97
Stepping	Leaf	14.57	14.49	31.56	4.19	8.30
	Z axis	26.73	36.28	49.20	5.89	12.35
Squatting	Leaf	10.75	11.59	34.83	7.56	23.20
	Z axis	50.06	57.01	77.71	11.40	29.10

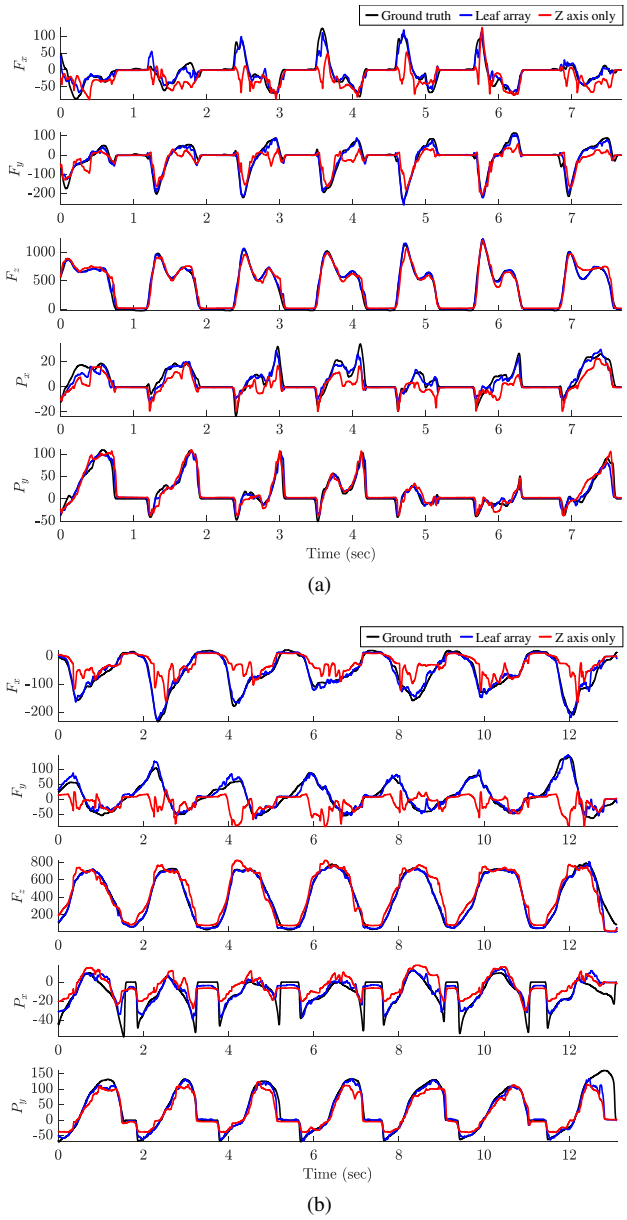

Fig. 9. The estimation results of GRF (F_x, F_y, F_z) and COP (P_x, P_y) comparing with using leaf FSR array and using only Z-axis information, during abnormal walking (a) and fastly repeated squatting (b).

The estimation results while abnormal walking and squatting are plotted in Fig. 9, and the RMS errors of each motion are presented in Table 1. It was observed that the accuracy that utilized information of vector-scaled three-dimensional force obtained from each array exhibited a minimum of twice and a maximum of five times greater accuracy across all types of movements compared to values derived using only z-axis information. In the case of the COP, the improvement in accuracy is not as substantial as in the case of GRF. This

means that while estimating the COP, the force ratio from the sensor modules placed on three distinct regions is more dominant than the direction of the forces.

IV. CONCLUSIONS

First of all, it has been confirmed that the three-dimensional force can be estimated using FSR sensors with the proposed leaf-inspired array. The limitations of FSRs in terms of single-axis measurements, considered one of their drawbacks, can be overcome by creating a multi-axis force sensor. Furthermore, by utilizing sufficient silicon layers, the low durability issue has been resolved. The nonlinearity and hysteresis are well compensated for linear vector scaling.

The GRF and COP were estimated with an accuracy of 4.8% using the estimated three-dimensional forces by utilizing a simple MLP. This paper, although conducted with data obtained from a single participant, suggests that the proposed sensor module can be used independently of the specific subject. The sensor's ability to measure three-dimensional forces with a single array was validated, and the experimental protocol included a process of measuring and normalizing pressure distribution in an upright posture. By not using a time window in the network's architecture, the learning of patterns inherent in time-series data was excluded. Training the network on various and irregular movements yielded a uniform improvement in accuracy when examining the output data, which included data along the x and y axes. Future research can establish protocols encompassing a wider range of movements, and validation across multiple subjects. In another way, using more advanced algorithms beyond the network training algorithm employed in this study could be a potential approach. Advanced architecture such as MobileNets [26] can be considered to further optimize the overall system performance.

REFERENCES

[1] G. Callaway, L. Field, X.-H. Deng, P. Torzilli, S. O'BRIEN, D. Altchek, and R. Warren, "Biomechanical evaluation of the medial collateral ligament of the elbow," *The Journal of Bone & Joint Surgery*, vol. 79, no. 8, pp. 1223–31, 1997.

[2] B. V. Hunter, D. G. Thelen, and Y. Y. Dhaher, "A three-dimensional biomechanical evaluation of quadriceps and hamstrings function using electrical stimulation," *IEEE Transactions on Neural Systems and Rehabilitation Engineering*, vol. 17, no. 2, pp. 167–175, 2009.

[3] K. A. Witte, J. Zhang, R. W. Jackson, and S. H. Collins, "Design of two lightweight, high-bandwidth torque-controlled ankle exoskeletons," in *2015 IEEE International Conference on Robotics and Automation (ICRA)*, pp. 1223–1228, 2015.

[4] A. Wu, X. Yang, J.-Y. Kuan, and H. M. Herr, "An autonomous exoskeleton for ankle plantarflexion assistance," in *2019 International Conference on Robotics and Automation (ICRA)*, pp. 1713–1719, 2019.

[5] S. Yu, T.-H. Huang, D. Wang, B. Lynn, D. Sayd, V. Silivanov, Y. S. Park, Y. Tian, and H. Su, "Design and control of a high-torque and highly backdrivable hybrid soft exoskeleton for knee injury prevention during squatting," *IEEE Robotics and Automation Letters*, vol. 4, no. 4, pp. 4579–4586, 2019.

[6] Y. Ding, M. Kim, S. Kuindersma, and C. J. Walsh, "Human-in-the-loop optimization of hip assistance with a soft exosuit during walking," *Science robotics*, vol. 3, no. 15, p. eaar5438, 2018.

[7] X. Liu and Q. Wang, "Real-time locomotion mode recognition and assistive torque control for unilateral knee exoskeleton on different terrains," *IEEE/ASME Transactions on Mechatronics*, vol. 25, no. 6, pp. 2722–2732, 2020.

[8] T.-H. Huang, S. Zhang, S. Yu, M. K. MacLean, J. Zhu, A. Di Lallo, C. Jiao, T. C. Bulea, M. Zheng, and H. Su, "Modeling and stiffness-based continuous torque control of lightweight quasi-direct-drive knee exoskeletons for versatile walking assistance," *IEEE Transactions on Robotics*, vol. 38, no. 3, pp. 1442–1459, 2022.

[9] S. K. Banala, S. K. Agrawal, A. Fattah, V. Krishnamoorthy, W.-L. Hsu, J. Scholz, and K. Rudolph, "Gravity-balancing leg orthosis and its performance evaluation," *IEEE Transactions on Robotics*, vol. 22, no. 6, pp. 1228–1239, 2006.

[10] H. Zhu, J. Doan, C. Stence, G. Lv, T. Elery, and R. Gregg, "Design and validation of a torque dense, highly backdrivable powered knee-ankle orthosis," in *2017 IEEE International Conference on Robotics and Automation (ICRA)*, pp. 504–510, 2017.

[11] C. Nabeshima, K. Ayusawa, C. Hochberg, and E. Yoshida, "Standard performance test of wearable robots for lumbar support," *IEEE Robotics and Automation Letters*, vol. 3, no. 3, pp. 2182–2189, 2018.

[12] S. J. Bamberg, A. Y. Benbasat, D. M. Scarborough, D. E. Krebs, and J. A. Paradiso, "Gait analysis using a shoe-integrated wireless sensor system," *IEEE Transactions on Information Technology in Biomedicine*, vol. 12, pp. 413–423, 7 2008.

[13] P. S. Dyer and S. J. M. Bamberg, "Instrumented insole vs. force plate: A comparison of center of plantar pressure," in *2011 Annual International Conference of the IEEE Engineering in Medicine and Biology Society*, pp. 6805–6809, IEEE, 2011.

[14] S. B. Joo, S. E. Oh, and J. H. Mun, "Improving the ground reaction force prediction accuracy using one-axis plantar pressure: Expansion of input variable for neural network," *Journal of Biomechanics*, vol. 49, pp. 3153–3161, 10 2016.

[15] H. S. Choi, C. H. Lee, M. Shim, J. I. Han, and Y. S. Baek, "Design of an artificial neural network algorithm for a low-cost insole sensor to estimate the ground reaction force (grf) and calibrate the center of pressure (cop)," *Sensors (Switzerland)*, vol. 18, 12 2018.

[16] T. Liu, Y. Inoue, and K. Shibata, "A small and low-cost 3-d tactile sensor for a wearable force plate," *IEEE Sensors Journal*, vol. 9, no. 9, pp. 1103–1110, 2009.

[17] J. Park, Y. Na, G. Gu, and J. Kim, "Flexible insole ground reaction force measurement shoes for jumping and running," in *2016 6th IEEE International Conference on Biomedical Robotics and Biomechatronics (BioRob)*, pp. 1062–1067, 2016.

[18] J. Park, S. J. Kim, Y. Na, Y. Kim, and J. Kim, "Development of a bendable outsole biaxial ground reaction force measurement system," *Sensors (Switzerland)*, vol. 19, 6 2019.

[19] J. Tao, M. Dong, L. Li, C. Wang, J. Li, Y. Liu, R. Bao, and C. Pan, "Real-time pressure mapping smart insole system based on a controllable vertical pore dielectric layer," *Microsystems and Nanoengineering*, vol. 6, 12 2020.

[20] S. Jang, J. Youn, S. Lim, S. Kim, U. Kim, and K. Kyung, "Development of a three-axis monolithic flexure-based ground reaction force sensor for various gait analysis," *IEEE Robotics and Automation Letters*, vol. 7, pp. 4118–4125, 4 2022.

[21] M. Hori, A. Nakai, and I. Shimoyama, "Three-axis ground reaction force distribution during straight walking," *Sensors (Switzerland)*, vol. 17, 10 2017.

[22] H. Choi and K. Kong, "A soft three-axis force sensor based on radially symmetric pneumatic chambers," *IEEE Sensors Journal*, vol. 19, no. 13, pp. 5229–5238, 2019.

[23] M.-C. Chiu, H.-C. Wu, and L.-Y. Chang, "Gait speed and gender effects on center of pressure progression during normal walking," *Gait & Posture*, vol. 37, no. 1, pp. 43–48, 2013.

[24] R. Jabbar, M. Shinoy, M. Kharbeche, K. Al-Khalifa, M. Krichen, and K. Barkaoui, "Driver drowsiness detection model using convolutional neural networks techniques for android application," in *2020 IEEE International Conference on Informatics, IoT, and Enabling Technologies (ICIoT)*, pp. 237–242, 2020.

[25] J. Xiao, J. Liu, H. Yang, Q. Liu, N. Wang, Z. Zhu, Y. Chen, Y. Long, L. Chang, L. Zhou, and J. Zhou, "Ulecgnet: An ultra-lightweight end-to-end ecg classification neural network," *IEEE Journal of Biomedical and Health Informatics*, vol. 26, no. 1, pp. 206–217, 2022.

[26] A. G. Howard, M. Zhu, B. Chen, D. Kalenichenko, W. Wang, T. Weyand, M. Andreetto, and H. Adam, "Mobilenets: Efficient convolutional neural networks for mobile vision applications," *arXiv preprint arXiv:1704.04861*, 2017.